Diagnosis of skin vascular complications revealed by time-frequency analysis and laser Doppler spectrum decomposition

Evgeny Zherebtsov, Igor Kozlov, Viktor Dremin, Alexander Bykov, Andrey Dunaev and Igor Meglinski *Senior Member, IEEE*

***Abstract*— Nowadays, photonics-based techniques are used extensively in various applications, including functional clinical diagnosis, progress monitoring in treatment, and provision of metrological control. In fact, in the frame of practical implementation of optical methods, such as laser Doppler flowmetry (LDF), the qualitative interpretation and quantitative assessment of the detected signal remains vital and urgently required. In the conventional LDF approach, the key measured parameters, index of microcirculation and perfusion rate, are proportional to an averaged concentration of red blood cells (RBC) and their average velocity within a diagnostic volume. These quantities compose mixed signals from different vascular beds with a range of blood flow velocities and are typically expressed in relative units. In the current paper we introduce a new signal processing approach for the decomposition of LDF power spectra in terms of ranging blood flow distribution by frequency series. The developed approach was validated in standard occlusion tests conducted on healthy volunteers, and applied to investigate the influence of local pressure rendered by a probe on the surface of the skin. Finally, in limited clinical trials, we demonstrate that the approach can significantly improve the diagnostic accuracy of detection of microvascular changes in the skin of the feet in patients with Diabetes Mellitus type 2, as well as age-specific changes. The results obtained show that the developed approach of LDF signal decomposition provides essential new information about blood flow and blood microcirculation and has great potential in the diagnosis of vascular complications associated with various diseases.**

***Index Terms*— Laser Doppler flowmetry, blood flow, microcirculation, optical Doppler effect, skin blood perfusion, Diabetes Mellitus.**

The authors acknowledge the support of the Academy of Finland (grants No. 318281, 326204). This work has also been partially supported by the European Union's Horizon 2020 research and innovation programme under grant agreement No.863214 - NEUROPA project, a grant under the Decree of the Government of the Russian Federation No. 220 of 09 April 2010 (Agreement No. 075-15-2021-615 of 04 June 2021) and the Ministry of Science and Higher Education of the Russian Federation, within the framework of State support for the creation and development of World-Class Research Centres, "Digital Biodesign and Personalized Healthcare" No. 075-15-2020-926 and Russian Foundation for Basic Research, project No. 19-32-90253. The collection of the clinical data was funded by the Russian Foundation for Basic Research (RFBR), grant No. 20-08-01153. The processing of the data from the heating test experiment was funded by the Russian Science Foundation, grant No. 20-75-00123 (Corresponding author: Evgeny A. Zherebtsov).

E. Zherebtsov is with the Opto-Electronics and Measurement Techniques, University of Oulu, Oulu, 90014, Finland and the R&D Center of Biomedical Photonics, Orel State University, Orel, Russia (e-mail: evgenii.zherebtsov@oulu.fi).

I. Kozlov is with the R&D Center of Biomedical Photonics, Orel State University, Orel, Russia (e-mail: igor57_orel@mail.ru).

V. Dremin is with the College of Engineering and Physical Sciences, Aston University, Birmingham, UK and the R&D Center of Biomedical Photonics, Orel State University, Orel, Russia (e-mail: v.dremin1@aston.ac.uk).

A. Bykov is with the Opto-Electronics and Measurement Techniques, University of Oulu, Oulu, 90014, Finland (e-mail: alexander.bykov@oulu.fi).

A. V. Dunaev is with the R&D Center of Biomedical Photonics, Orel State University, Orel, Russia (e-mail: inohvat@yandex.ru).

I. Meglinski is with the Opto-Electronics and Measurement Techniques, University of Oulu, Oulu, 90014, Finland; Institute of Clinical Medicine N.V. Sklifosovsky, I.M. Sechenov First Moscow State Medical University, Moscow, Russia; Institute of Engineering Physics for Biomedicine, National Research Nuclear University (MEPhI), Moscow, Russia; Immanuel Kant Baltic Federal University, Kaliningrad, Russia; Interdisciplinary Laboratory of Biophotonics, Tomsk State University, Tomsk, Russia. He is now with the College of Engineering and Physical Sciences, Aston University, Birmingham, UK (e-mail: i.meglinski@aston.co.uk).

I. Introduction

THE use of optical methods for the characterisation of biological tissue parameters is a dynamically developing area of medical diagnostics. Modern light sources combine high-quality parameters of coherence with excellent power efficiency at an affordable cost. Such techniques as dynamic light scattering (DLS) and laser Doppler flowmetry (LDF) utilise the properties of laser light. A group of methods are demonstrated for use in the retrieval of important information about the structural features of living tissue, capillary blood flow and microvascular properties [1]. Quantitative characterisation of the size, concentration and mean speed of scattering particles in the media becomes possible with interpretation of the measurement information obtained by the effect of quasi-elastic DLS. Although the theory of DLS has been developed in sufficient depth, there is a knowledge gap between mathematical modelling and the practical applications of the methods of clinical diagnostics. The diagnostic capabilities, metrological certification, and scope of applications of this medical technology are still at the development stage [2].

In biomedical diagnostics, DLS and LDF are used mainly for blood flow characterisation in the superficial layers of skin and mucosa. The LDF technique allows one to estimate the blood flow in the microvasculature *in-vivo* with high

temporal resolution. The method is based on optical non-invasive sensing of tissue using laser light and further analysis of the scattered radiation partially reflected by the moving red blood cells. Classic LDF theory in the approximation of quasi-elastic light scattering measurement of blood flow in tissue microvasculature suggests that the first moment of the photocurrent power spectrum $S(f)$ of the photodetector varies directly with relative blood flow (blood perfusion, PU): $I_m = \int_{f_1}^{f_2} f \cdot S(f) df$. Where the blood flow is described as the product of the blood cell concentration and mean speed. The frequency limits f_1, f_2, for practical purposes, are selected from the range $60 - 20000\ Hz$, which closely corresponds to the physiological range of the mean blood velocity in the superficial layers of the skin $(0 - 10\ mm/s)$ [3], [4].

The LDF method has its origins in early publications which substantiated the registration of the Zeeman wavelength-splitting bandwidth of radiation in a magnetic field by means of the photomixing effect on a light-sensitive element [5]. Further, after several publications, it has been substantiated that this effect can be used for non-invasive registration of flow characteristics [6] and subsequently microcirculation [7]–[9]. Microcirculatory blood flow exhibits vasomotions, which are rhythmic oscillations in vascular tone, caused by changes in smooth muscle constriction and dilation. This phenomenon is controlled locally, as well as systemically. Harmonic analysis of rhythmic oscillations in the fine structure of microvascular blood flow increases the diagnostic significance of the LDF method. Time series recordings of LDF signals allow discrimination of blood perfusion modulation rhythms originating from the heart $(0.6-2\ Hz)$, respiratory $(0.145-0.6\ Hz)$, myogenic $(0.05-0.15\ Hz)$, neurogenic $(0.02-0.5\ Hz)$ and endothelial $(0.005-0.02\ Hz)$ physiological and vascular activities in the organism [10], [11]. These modulation amplitudes provide valuable information about microvascular tonus. In the late 90s and early 00s, the work of Stefanovska's group and others substantiated the study of microcirculation rhythms based on wavelet transforms [12]–[14], which carry essential diagnostic information. Insufficient performance of these rhythms is indicative of the development of complications of diseases such as diabetes [15], [16] and rheumatic diseases [17]. The occlusion test, cold pressor test and orthostatic test have also been combined with LDF recordings, demonstrating significant improvements in sensitivity and specificity in the discovery of microvascular diseases [18]. In addition, aspects of the application of LDF in dentistry have become a separate scientific field. Because of its ability to assess blood flow non-invasively, LDF is now in demand for the diagnosis of gingival inflammation [19], the quality of therapy [20], and the pulp blood flow [21]. LDF has also found an application in the tasks of diagnosing the damage recovery process, such as in Achilles tendon injuries [22]. Microcirculation studies are also important in free-flap surgery for analysis of engraftment and restoration of blood supply [23], as well as in burn wound healing [24]. A special area of interest for the LDF is the development and application of wearable LDF devices. The possibility of distributed registration of microcirculation simultaneously from various areas (wrists, legs, forehead) opens up possibilities for studying the phase and amplitude coherence of blood flow for a range of external conditions and functional tests. Wearable LDF design allows this method to be used for monitoring of microcirculation during active movement of a subject [25].

The shape of the Doppler broadening spectrum obtained from the scattering of particles moving with constant velocity can be described by a Gaussian function [26]. In fact, the shape of the resulting spectra may be far from Gaussian in the case of blood microflow within the skin. The contribution of each sub-band of RBC velocities to the overall estimated blood perfusion may vary significantly. Apart from the velocity variations of RBC, the fluctuations in their concentration in the diagnostic volume should be taken into account. The blood flow is evaluated as a product of the average speed and the density of flowing RBCs scattering light. The diagnostic information of the exact reason for the observed changes in the registered blood flow is hidden by uncertainty after the integration of all physiologically relevant frequencies of the Doppler power spectrum.

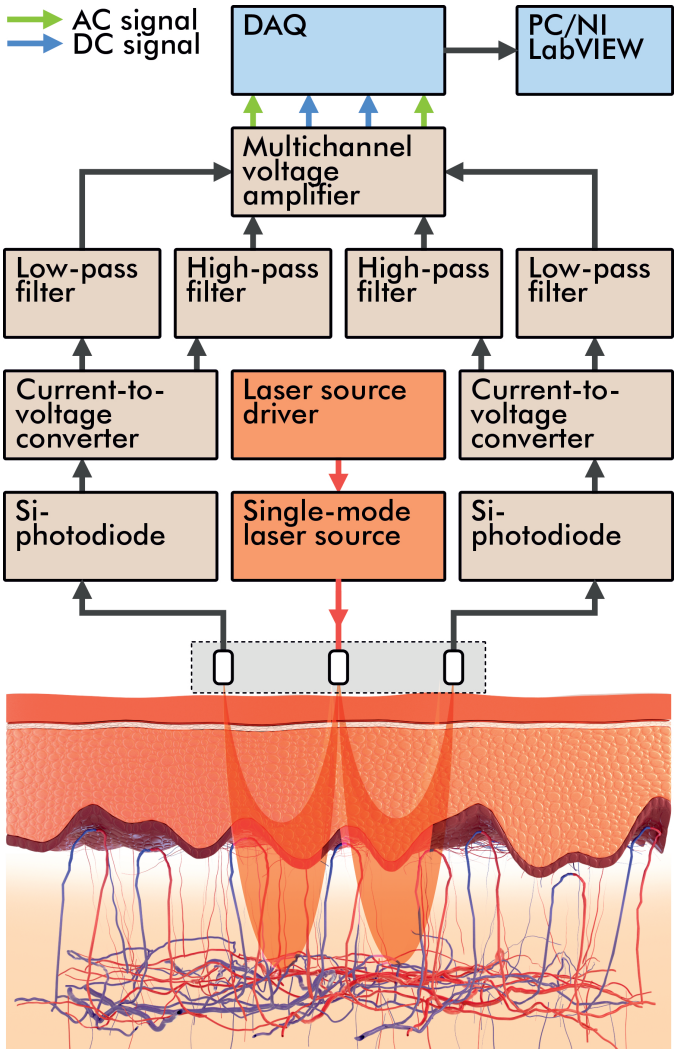

Fig. 1. Flowchart of the developed experimental setup for LDF measurements.

One of the promising developments in laser Doppler blood perfusion monitoring is the separate analysis of the power spectrum components calculated from the digitised photocurrent time-series. This data may contain useful information, such as estimation of the velocity and scattering phase function of moving particles [27]–[29]. In 1993, Obeid [30] observed that the processing bandwidth of integration over frequencies of Doppler spectra corresponds with a range of speed components of the flowing liquid. That effect was applied for the analysis of the blood flow in dental pulp, demonstrating that processing bandwidth with a cut-off frequency of $3000\ Hz$ is more effective and has a better signal-to-noise ratio than using a wider bandwidth [31], [32]. Also, an important role of Doppler spectra correction was described in 2004 [33]. In these studies, the authors proposed that the fine tuning of the frequency range can minimise the influence of biological zero and reject white noise [34].

Three types of occlusion test were used to distinguish blood flow in different vascular beds by analysis of laser Doppler frequencies [35]. The resolution of the LDF approach towards measurements of velocity distribution was evaluated in several types of blood vessels [36], [37]. The development of LDF processing techniques and instrumentation was supported by clinical studies that suggested the use of the LDF method resolved uncertainty regarding the velocity components of the skin blood flow [38], [39]. Thus, not only amplitudes but both the shape of the power spectrum and its frequency distribution carry substantial physiological information with valuable diagnostic potential.

This study hypothesised that the combined selection of the frequency ranges in blood perfusion oscillations and the Doppler broadening spectra can significantly increase the accuracy of detecting pathological changes in blood microvessels. For the first time, to the best of our knowledge, we introduce a new signal processing approach for the decomposition of blood flow microvascular oscillations in terms of their allocation by frequencies of Doppler shift and validate the method in the standard physiological tests and limited clinical trials.

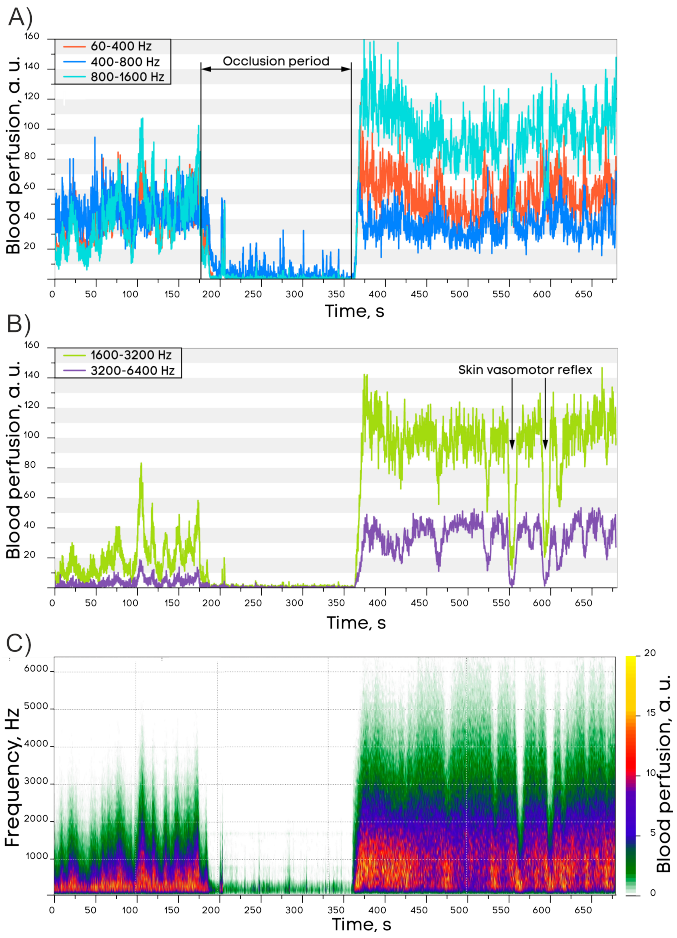

Fig. 2. Example of LDF signals recorded in frequency sub-bands (A) 0—400 Hz, 400–800 Hz, 800–1600 Hz; (B) 1600–3200 Hz, 3200–6400 Hz. (C) Visualisation of index of microcirculation by frequency of Doppler shift in the experiment.

II. Material and Methods

A. Experimental LDF system and data processing

Commonly, blood perfusion measured by LDF is the result of photocurrent processing from a photodetector produced by photomixing of optical fluxes with the reference and Doppler-shifted ($<24\ kHz$) components [40]. The reference component is formed by light scattered and reflected from non-moving tissue structures. Epidermis and cutaneous structural proteins like collagen and elastin are involved in the formation of the reference component [41], whereas moving particles, mainly erythrocytes, are responsible for the formation of Doppler components. Subtraction of one signal allows for artefacts of different kinds to be reduced. At the next step, the power spectrum of the digitised signal is computed and the amplitude value of the spectrum is multiplied on the corresponding Doppler shift frequency. The square of the DC component of the photocurrent is usually utilised as the normalising coefficient. In case of the conventional processing algorithm assuming integration by a wide frequency range, the vastness of the important information about signal distribution by the power spectrum can be lost. In this study, we investigate the benefits of the blood perfusion calculation in narrow ($100-200\ Hz$) frequency sub-bands of the power spectrum, with subsequent harmonic analysis of the time-series recordings. We have developed an in-house built setup capable of comprehensive characterisation of the blood perfusion alterations in living tissues and flexible analysis of the power spectrum redistribution in different sub-bands of the Doppler shift. A flowchart of the setup is presented in Fig. 1.

In the measuring channel, a single-mode laser (LPS-785-FC, Thorlabs, USA) with $785\ nm$ wavelength and $2\ mW$ of output power was utilised as a radiation source. A fibre optical probe coupled with the laser delivered radiation to the skin surface and collected backscattered light to be converted to photocurrent by two Si-photodiodes. The received signal was amplified by an electronic board with current-to-voltage converter and low- and high-pass filters separating the AC and DC components of the electrical signal. The analog-to-digital conversion was performed by a data acquisition board model NI USB 6211 (National Instruments, USA). Signal

processing was conducted on a PC with the NI LabVIEW environment. Two photodiodes and two independent signal processing channels made it possible to operate with the different signals to remove the common-mode artefacts and non-informative signal components.

The core of the signal processing procedure implemented in the virtual instrument was carried out according to the classical expression [40], [41]:

$$I_m = \frac{\int_{f_1}^{f_2} f \cdot S[U1(t) - U2(t)]df}{i_{dc}^2}, \quad (1)$$

where $S[U1(t) - U2(t)]$ is the power spectrum of the resulting recording retrieved from the subtraction of the AC signals of the two photodetectors; i_{dc} is the average DC signal from the two sources. The power spectrum was calculated by the standard virtual instrument in the LabVIEV environment. The sampling rate of the raw input signal was $50\ kHz$, with a sampling length of 5000 samples each [42]. With these settings, the power spectra were calculated and recorded at the rate of 10 spectra per second.

The amplitude spectra of the perfusion oscillations corresponding with the Doppler frequencies was calculated according to the following procedure. First, the obtained stack of power spectra was sliced into sub-bands with a step of $200\ Hz$. Next, the perfusion value was calculated for each frequency band by the Eq. 1. Finally, the time series of blood perfusion computed in the frequency sub-ranges was processed with a wavelet transform to obtain an integral wavelet spectrum.

The wavelet transform $W_x(f_{osc}, \tau)$ of a blood perfusion time-series $I_m(t)$ is defined in terms of the appropriate mother wavelet $\psi(t)$, as given in Eq. 2:

$$W_x(f_{osc}, \tau) = \sqrt{f_{osc}} \int_{\infty}^{\infty} I_m(t)\psi^*[f_{osc}(t - \tau)]dt, \quad (2)$$

where t is the time, τ is the time shift of the wavelet, f_{osc} is an estimate of the oscillation frequency ($\sim 1/a$, where a is the time-scale of the wavelet), and the symbol * indicates the operator of complex conjugation. We utilise here the Morlet wavelet [43]:

$$\psi(t) = e^{2\pi i t} e^{-t^2/2\sigma^2}. \quad (3)$$

The Morlet wavelet is one of the commonly used wavelets, which allows examination of the amplitude and phase properties of oscillations of different frequencies in the signal. The integrated wavelet spectrum was calculated by integrating of Eq. (2) over period T as follows:

$$M_{osc}(f_{osc}) = \frac{1}{T} \int_0^T |W_x(f_{osc}, \tau)|^2 d\tau. \quad (4)$$

Since the time-series of $I_m(t)$ is calculated within frequency limits of signal integration (f_1, f_2) with some central frequency $f_D = (f_1 + f_2)/2$, the integrated wavelet spectrum can also be treated as a function of parameter f_D: $M_{osc}(f_{osc}, f_D)$.

Thus, for one measurement, after the signal processing routine is applied, we obtain a matrix:

$$M_{osc} = \begin{bmatrix} a_{11} & \dots & a_{1M} \\ \vdots & \ddots & \vdots \\ a_{K1} & \dots & a_{KM} \end{bmatrix}, \quad (5)$$

where K is the number of elements in the vector of discretised Doppler shift frequencies f_D, M is the number of elements in the vector of blood perfusion oscillations f_{osc}. In this study, the dimensions of the matrices of blood perfusion oscillations were equal for all measurements where this analysis was applied. To identify the ranges of Doppler frequencies f_D and the frequencies of the blood perfusion oscillations f_{osc} that would have better diagnostic significance in separating the experimental samples of patients and volunteers, we calculated maps of the distribution of p-value by the Mann-Whitney U-test. The test was performed over all points with the given coordinates of $M_{osc}(f_{Dk}, f_{osc_m})$ over the data obtained in the groups of healthy volunteers, as well as patients with type 2 diabetes mellitus (DM). The image map of the p-values is coloured in pseudocolours ranging from 0 to 1. The lowest values correspond to the statistically significant difference in the amplitude of the blood perfusion oscillations in the region of the frequencies. According to these maps, we identified areas of interest to further calculate the feature space and build the diagnostic testing classifier. The first variable (area 1) of the input vector was the sum of amplitudes over the rectangular with limits of $f_{osc} \in (0.08\ Hz, 0.7\ Hz)$ and $f_D \in (800\ Hz, 7000\ Hz)$. The second variable (area 2) had limits of $f_{osc} \in (0.8\ Hz, 2\ Hz)$ and $f_D \in (5000\ Hz, 12800\ Hz)$ accordingly. The highlighted areas correspond to the neurogenic and myogenic oscillations (area 1) and localisation of cardiac oscillations (area 2). To estimate the effects of selection by a range of Doppler frequencies, we compared one with the amplitudes integrated over all values of the available Doppler shift range for the same frequency span of blood flow oscillations.

B. Functional tests

At the first stage, we verified the proposed approach in a series of tests with standard functional tests, proven to be able to alternate the skin blood flow in a predictable and reproducible manner. To verify the hypothesis that significant changes of the blood flow are accompanied by the redistribution of the calculated blood perfusion over frequencies of the Doppler spectra, we used the arterial occlusion test [44]. The applied occlusion allowed us to estimate the level of the registered blood perfusion signal when the blood flow in the skin was blocked. Also, in normal conditions, the test reliably provokes skin hyperaemia and increases the blood perfusion during the time immediately after the occlusion is released.

The arterial occlusion was performed on the upper arm using a sphygmomanometer air cuff with a pressure of $220\ mmHg$. Fourteen healthy volunteers with an average age of $21\ years$ participated in the experimental part. During the test, the fibre optical probe was placed on the middle finger pad and the blood perfusion recordings by the LDF setup

were registered by the integration of the power spectra in the following frequency sub-bands: 60–400 Hz; 400–800 Hz; 800–1600 Hz; 1600–3200 Hz; 3200–6400 Hz. At the stage of signal processing and visualisation, the full analysed range was limited to frequencies in the range of 60–6400 Hz. The preliminary evaluation of the relative impact of the signal from the higher frequencies [45], [46] was admitted to have an insignificant impact on the clarity and conclusions of the implemented experimental studies. Every experiment was conducted following the protocol: recording of the basal level of blood perfusion (3 min); occlusion test (3 min); post-occlusion recording (5 min).

A step-wise increase in local pressure is known to cause a gradual change in the parameters of capillary blood flow in the upper layers of the skin, and can also affect the measurement results of various optical methods [47]–[49]. The impact of the procedure has several subsequent effects, such as mechanical compression of vessels, and neurological and metabolic compensating mechanisms like pressure-induced vasodilation, which maintain the homeostasis of the skin during moderate levels of external pressure and tissue hypoxia [50]–[52]. To examine how those effects are translated to the blood flow registering in different ranges of the Doppler spectra, we have developed a 3D-printed pressure distribution tool (PDT) compatible with the fibre-optical probe which was used, and equipped with a set of weights. The experimental series was conducted on the dorsal surface of right middle finger with the PDT placed coaxially to the probe (Fig. 3).

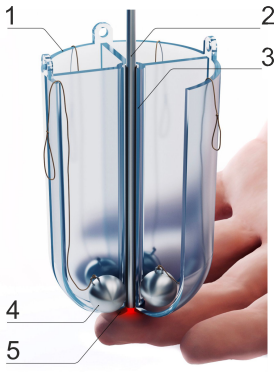

Fig. 3. 3D-printed pressure distribution tool coaxially allocated to the fibre optical probe. 1 – pressure distribution tool; 2 – fibre-optical probe 3 – central guide tube for the probe; 4 – lead weights; 5 – tip of the fibre-optical probe.

During the main series of measurements, the weights were placed into the PDT in a step-wise manner to achieve the following values of pressure applied: 10 $mmHg$, 30 $mmHg$, 90 $mmHg$, 150 $mmHg$, 210 $mmHg$. At the end of the procedure, the load was reduced back to 30 $mmHg$. Experiments were conducted with the participation of 7 healthy volunteers with 10 min LDF recording for each step. To estimate the prominence of the observed effects and substantiate the measuring routing, several preliminary experiments were also conducted where the set of values of pressure was applied with a step-wise increase and then decrease with about 2 min of LDF recordings for each step.

C. Trial measurements in patients with DM type 2

Finally, the experimental setup with the proposed signal processing was tested in a series of clinical trials involving two cohorts of conditionally healthy volunteers of different ages and patients with type 2 diabetes. As the area of interest, the dorsal surface of the foot was chosen. In this study, to maximise the difference in vascular response, a heat test was used. Moderate skin heating was applied by a metal pad adjusted to a water-cooled Peltier element, coaxially assembled with the fibre-optical probe of the LDF channel. The location of the probe on the volunteer's foot is shown in Fig. 5A. The measurements were performed at least 2 h after caffeine intake and meal with 15 min acclimatisation to the room conditions.

TABLE I
CHARACTERISTICS OF T2DM PATIENTS AND VOLUNTEERS

Parameters	Patients	Group 1	Group 2
Age (y)	61±7*	21±0.7*	50±7*
Sex (M/F)	4/7	5/5	3/4
Systolic BP (mmHg)	125±11	120 ± 7	118±4
Diastolic BP (mmHg)	75±7	71±4	75±3
Body mass index (kg/m^2)	31±4.5*	24±2.5	23±3
Fasting glucose (mmol/l)	10.4±3	-	-
Diabetes duration (y)	11.5±4	-	-
HbA1c (%)	7.1±0.2	-	-
Total cholesterol (mmol/l)	5.2±0.8	-	-
Creatinine (μmol/l)	78.6±7.6	-	-
Urea (mmol/l)	6±0.9	-	-
ALT (IU/L)	24.9±5.4	-	-
AST (IU/L)	19.9±4.3	-	-

Note: Data in the columns is represented as mean±SD except Sex parameter. Reference values of the laboratory: HbA1c 4.0% to 6.0%, total cholesterol 3.5 to 5.0 mmol/l, urea 2.5 to 7.5 mmol/l, creatinine 70 to 110 μmol/l, ALT 10 to 38 IU/L, and AST 10 to 40 IU/L. * – denotes a statistical difference identified by Mann-Whitney U-test, $p < 0.05$.

The criterion for inclusion of a patient in the group was the absence of the following complications: toe amputations, lesions, necrosis, and diabetic foot syndrome. The groups of healthy volunteers were formed based on the absence of diagnosed cardiovascular diseases and the absence of antidepressant medications. The LDF signal was recorded according to the protocol, divided into three stages. The first stage (stage 1) involved 10 min measuring the blood perfusion baseline at the Peltier element temperature of 33°C. At the second stage, the local temperature was increased step-by-step at the rate of 2°C per minute to 42°C. At the third stage, blood perfusion evolution during thermal stimuli was recorded for 20 min. The design of this protocol is based on the fact that nociceptive C-fibres are activated and endothelial vasoactive substances are released at about 42°C temperature exposition with subsequent changes in the skin blood perfusion.

Cohorts of volunteers included three groups: 7 non-smoking volunteers (22 ±0.5 $years$; 6 volunteers aged 51 ±0.5 $years$; 11 non-smoking volunteers (61 ± 7 $years$) with type 2 diabetes confirmed for at least 5 $years$. The criteria for inclusion in the sample were the absence of diabetic foot, necrosis and lesions. The necessary information about the patient group in the study is shown in Table 1. The studies with the

participation of volunteers were conducted according to the guidelines of the Declaration of Helsinki, and approved by the Ethics Committee of Orel State University (Minutes No. 15 dated 21 February 2019).

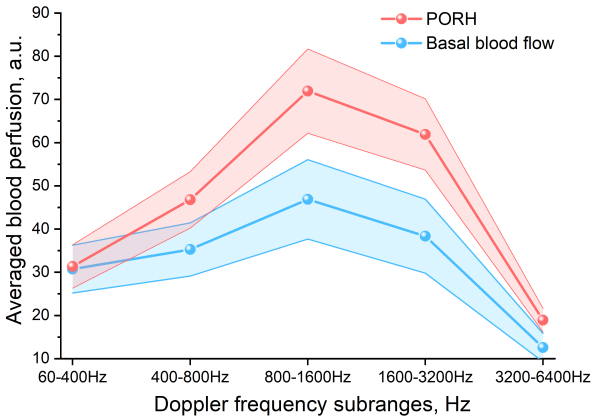

Fig. 4. Skin blood perfusion calculated in the frequency sub-bands before applying (basal blood flow) and immediately after releasing the upper arm arterial occlusion (PORH – post-occlusive reactive hyperaemia). The results are averaged over n = 14 experiments; a single SE is taken to show scattering.

III. Results and Discussion

A. Occlusion test

Relevant examples of the LDF signals recorded by the selected frequency sub-bands during the occlusion test are presented in Fig. 2. Time intervals $50\ s$ before occlusion and $15\ s$ immediately after the occlusion removal were selected to estimate the average values of the perfusion for every frequency range and their scattering. The combined profiles of the average perfusion in the selected frequency sub-bands before and after the occlusion are shown in Fig. 4. From the plots, it can be seen that the main component of the blood perfusion increase is the signal with the Doppler frequency shift from the range of $400-3200\,Hz$, while the $60-400\,Hz$ and $3200-3200\,Hz$ sub-bands bring minor impact to the total signal. It can be seen also that the $800-1600\,Hz$ frequency span contributes the most to the peak of reactive hyperemia.

As can be seen from Fig. 2 the uncertainties and variability of skin blood perfusion calculated in the frequency sub-bands of Doppler shift frequencies vary significantly, depending on the Doppler frequency subrange of the signal integration. For the experiment with measurements of blood perfusion before applying and immediately after releasing the upper arm arterial occlusion, the highest scattering of data was observed in the subrange of $800-1600\,Hz$ with an average perfusion of $46.9 \pm 9.1\,a.u.$ and $71.9 \pm 9.7\,a.u.$ before and after occlusion, respectively. For the frequency subrange of $60-400\,Hz$, the results of measurements are $30.7 \pm 5.5\,a.u.$ and $31.3 \pm 5.0\,a.u$, and for the subrange of $3200-6400\,Hz$: $12.5 \pm 3.2\,a.u.$ and $18.9 \pm 2.7\,a.u.$ respectively. From that, we can conclude that the variability of the blood perfusion measurements does not change significantly before and after the occlusion. The observed scattering of experimental data comprises both instrument errors and the physiological variability of the measurable parameters from person to person.

In addition, in Fig. 2A, Fig. 2B, relevant examples of the skin vasomotor reflex can be seen. The observed signals are linked to the spasmodic effect of the microvascular system, localised in local frequency sub-bands. The decrease in higher-frequency sub-bands (see Fig. 2A) is accompanied by a substantial increase in blood perfusion recordings, calculated in the low-frequency range (see Fig. 2A). The observed effect supports the hypothesis that the speed profile redistribution of the moving RBCs causes a scalable redistribution of the power spectrum of the raw LDF signal from the photodetector. A decrease in the fraction of fast RBCs is followed by an increase in the lower speed fractions. It should be mentioned that not only blood components but also scattering from lymph contributes to the total registered perfusion. It is known that the lymphatic microcirculation is closely related to venous blood flow [53]. Therefore, a reflective lymph-based signal is likely to overlap with the LDF signals in the low-frequency spectral band [54], [55].

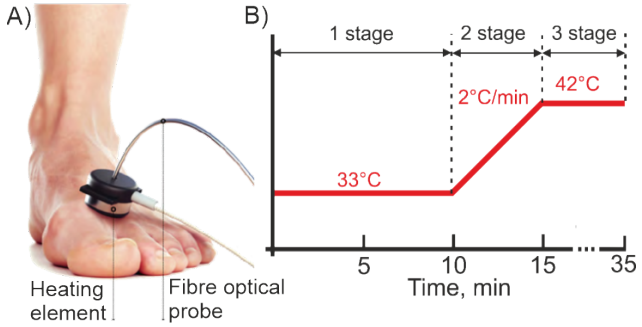

Fig. 5. (A) Location of the fibre optical probe on the volunteer's foot; (B) Study protocol with the heat test.

The calculation of the blood perfusion from narrow frequency ranges of the Doppler power spectrum allows us to introduce here a more informative way of visualising an LDF blood perfusion time-series recording. An example of the representation of the signals from Fig. 2A and Fig. 2B is shown in Fig. 2C. Here, in one plot, the distribution of perfusion is presented in two dimensions of time and corresponding Doppler frequency. The time-series of the signal allows the visualisation of non-stationary changes in the blood flow, while the alterations in the estimated blood flow over the Doppler frequencies is connected to the changes in the histogram of the RBC speed distribution. This type of plot greatly benefits from the instant possibility of visualising the contribution of every component of the blood flow to the total registered blood perfusion.

Among other components, Fig. 2C demonstrates the spectral pattern of the LDF signal during the time interval when the occlusion is applied. The phenomenon of a continuing blood perfusion signal when associated cardiac activity blood flow is blocked is widely known as biological zero (BZ). The signal originates from the Brownian motion of the RBCs and the residual blood flow caused by the redistribution of pressure among microvessels when the arterial occlusion is applied [56], [57]. Motion artefacts due to the tremor of

the occluded limb may also interfere with the measurements. As can be seen from Fig. 2C, the signal of BZ is mainly localised in a relatively narrow band of low Doppler shift frequencies. The blood perfusion time-series calculated over Doppler components exceeding 1600 Hz demonstrate a very minimal level of signal during occlusion. In contrast, the spectral region of 400-1600 Hz carries most of the energy of the Doppler signal under these conditions, resulting in a substantial perfusion signal associated with BZ. Electrical noise, including white noise with a broad spectrum, also affects the resulting calculated perfusion signal. The common way to reduce its influence is to limit the frequency range of the digitised signal by informative frequencies, containing information about the blood perfusion and suppress all non-informative frequencies.

B. Test with local pressure

A representative example of the blood perfusion measurements during the loading and uploading application of pressure to the probe is shown in Fig. 6. With an increase in the pressure, the frequency bandwidth of the blood perfusion allocation over the Doppler shift begins shrinking. It should be noted that the decrease is followed by an increase in the spectral density of the estimated perfusion in the lower frequency spectral ranges. This effect can be explained by a reasonable assumption that, in a, certain range, the increased pressure slows the speed of RBCs, while the total amount of the dynamically scattering elements in the sampling volume of the fibre-optical probe does not change significantly. This leads to an increase in the amplitude of the blood perfusion signal located in the low frequency sub-bands of the Doppler shift and drastically decreases it in sub-bands of higher frequency. Once the pressure is completely blocking the major components of the blood flow, the signal of blood perfusion seems to be suppressed almost completely. The observation of the shape and behaviour of blood perfusion distributed over the Doppler shift frequencies has led us to the hypothesis that the gradual increase of the pressure has a different impact on the blood flow oscillations in the minor blood vessels in the sampling volume of the fibre-optical probe. The remaining spikes of the blood perfusion at the higher levels of mechanical pressure are very likely associated with cardiac activity and the systolic pulse wave. To study the effect, we conducted an extended series of measurements when the mechanical pressure probe changed to 10 $mmHg$, 30 $mmHg$, 90 $mmHg$, 150 $mmHg$, 210 $mmHg$ and again 30 $mmHg$ at the last stage. The blood perfusion was recorded for 10 min at each stage.

The longer time-series allowed us to figure out not only the average value of the blood perfusion but also the wavelet spectrum of the physiological oscillations for every 200 Hz constituent Doppler frequency sub-band with the identification of the cardiac (C), respiratory (R), myogenic (M), neurogenic (N) and endothelial (E) rhythms. The obtained distributions of the oscillation amplitudes over the dimensions of their frequency, as well as the corresponding Doppler shift frequency, were calculated for each level of pressure applied to the probe. The 3D plots averaged over data from 7 volunteers are shown in Fig. 7 (interpolated and smoothed).

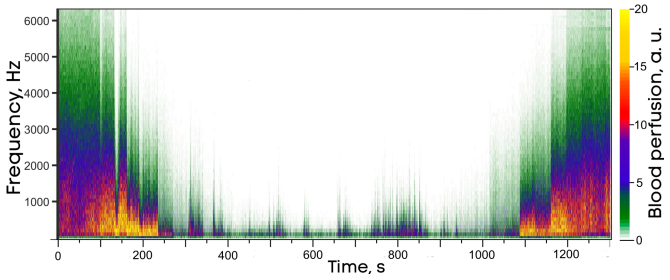

Fig. 6. A relevant example of the distribution of calculated blood perfusion by frequency of Doppler shift for local pressure.

The evaluated characteristics of perfusion distribution may contain valuable new information about the parameters of skin blood flow. From Fig. 7, it can be seen that the gradual increase in pressure depletes the ensemble of microvascular oscillations, beginning mostly from the low frequencies (M, N, E oscillations) while cardiac oscillations remarkably keep or even increase their amplitude in the area of lower frequencies of the Doppler shift (Fig. 7C, Fig. 7D and Fig. 7E). Nevertheless, at probe pressures higher than the systolic blood pressure, the oscillation amplitudes in the Doppler spectral ranges higher than 5 kHz drop almost to the level of noise, with a minor remaining cardiac peak. This observation also confirms the redistribution of the speed of RBCs during the pressure test, as well as substantiating the ability of the proposed technique to reliably detect and quantify the effect. Interestingly, the transient from the $P = 10\ mmHg$ to $P = 30\ mmHg$ is accompanied by an increase of the cardiac, myogenic and neurogenic oscillations, which can be explained by the effect of pressure-induced vasodilation. After the pressure dropped from $P = 210\ mmHg$ to $P = 30\ mmHg$, the parameters of blood flow did not recover to the earlier level, suggesting the presence of significant hysteresis in the analysed processes. Here, we should also consider the effect of the optical clearing of the compressed, whitened skin. Once the compression rises, the sampling volume of the fibre-optical probe also increases, reaching deeper skin layers, populated with arterioles, where the cardiac oscillations dominate the most [58].

C. Trial measurements in patients with DM type 2

The intriguing and promising results from the verification of the presented technique in functional tests in healthy volunteers suggested we should proceed with limited clinical trials to evaluate its potential diagnostic significance. The unequal distribution of the blood perfusion oscillations over the frequencies of Doppler broadening imply a variation in their diagnostic value. The conscious selection of Doppler shift ranges has the potential to increase the accuracy of the diagnostic classifiers implemented on their basis. To verify this assumption, for the maps obtained of perfusion oscillation distribution (Fig. 8), measured in diabetic patients and volunteers of the two age groups, the p-value parameter was evaluated by the Mann-Whitney statistical test. The maps of p-value were used to estimate areas of the microvascular oscillations where the difference of the blood flow oscillations between the

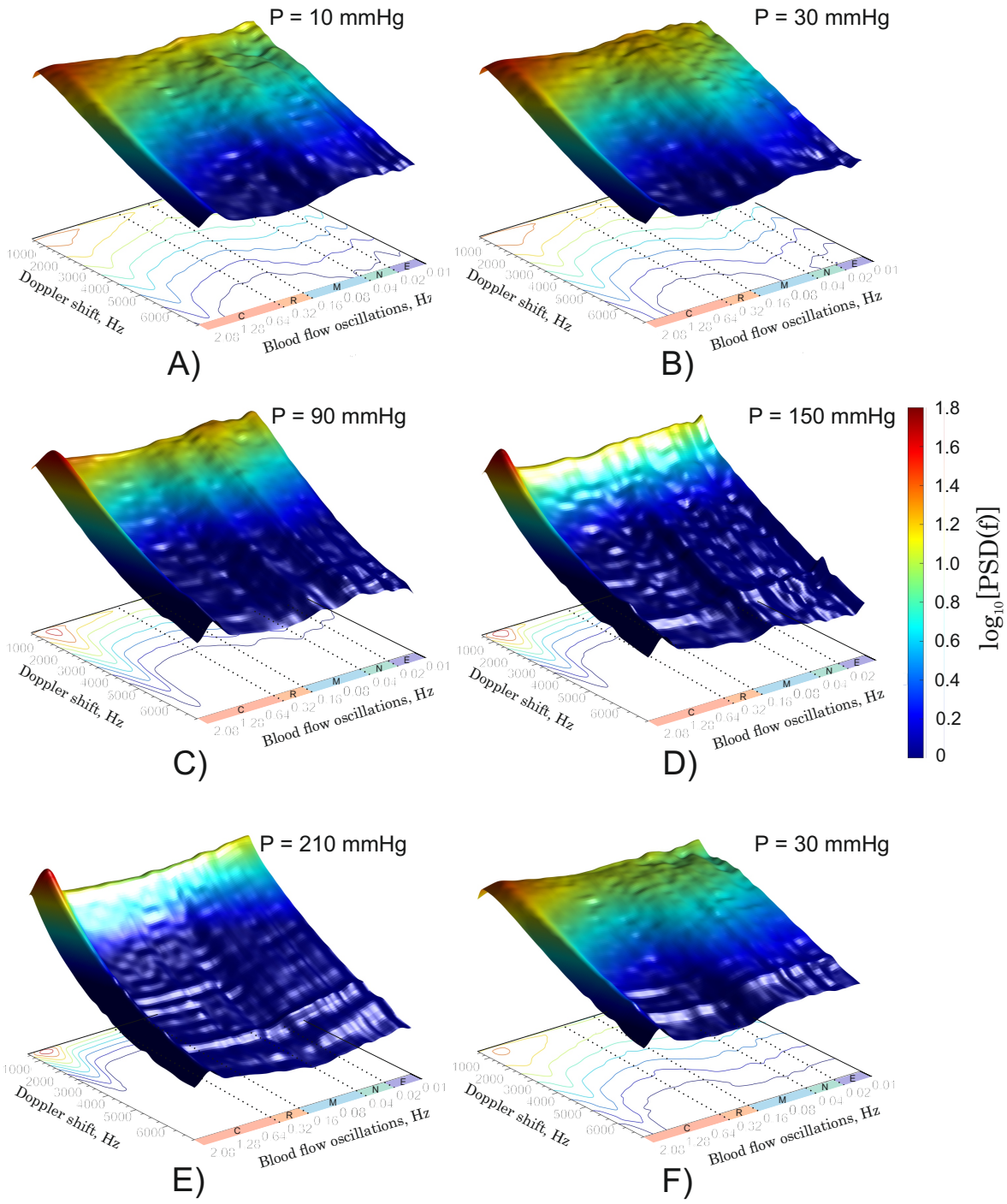

Fig. 7. Mean distribution of blood flow oscillation across the Doppler shift evaluated by the proposed approach with local pressure test. A – stage 1 (10 mmHg), B – stage 2 (30 mmHg), C – stage 3 (90 mmHg), D – stage 4 (150 mmHg), E – stage 5 (210 mmHg), F – stage 6 (30 mmHg).

separate groups in the 2D frequency space considered was the highest (see Fig. 9). For the first demonstration, and to simplify the task but prove the principle, we selected the rectangular areas in the space with minimised p-value and calculated the integral amplitudes within them. In the selection of the areas, we aimed at better delineation of the patients from the both groups of volunteers. Nevertheless, we also considered the opportunity to identify the changes due to ageing, using the same selected areas. To compare the new approach, we calculated the amplitudes in the same frequency range of blood flow oscillations without filtering by the Doppler frequencies, thus implementing the classical approach in which the blood perfusion is calculated by integration over the full frequency range. p-value maps were calculated for stages 1 and 3, but the difference between the delineating groups was much more prominent after applying the thermal test. For that reason, the data from stage 3 were used for the final analysis.

To form the input vector taking into account the limited set of measurements conducted, two regions were chosen, corresponding to myogenic and respiratory activity (region 1)

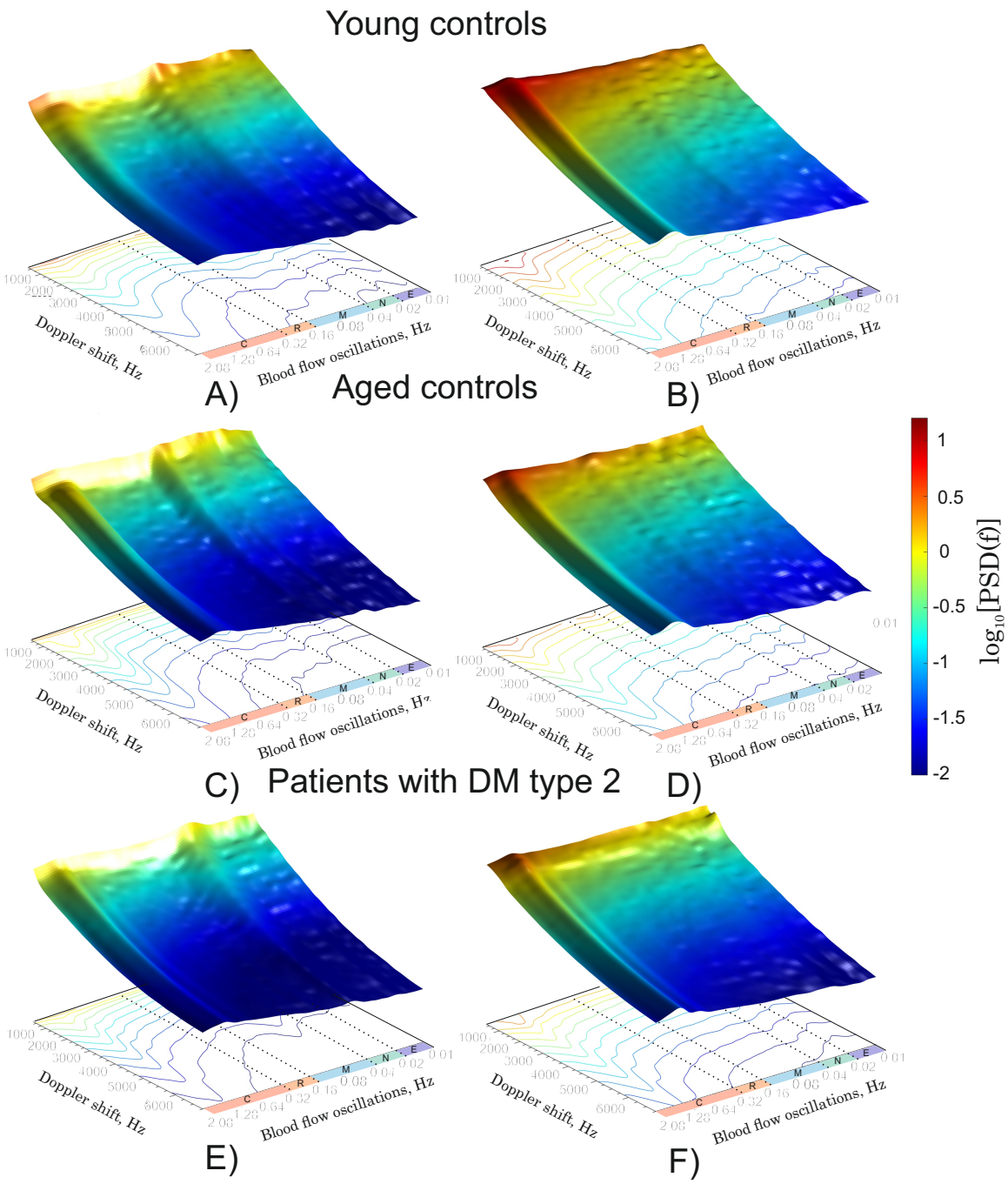

Fig. 8. Mean distribution of blood flow oscillation across the Doppler shift before and after heating test in healthy volunteers of two age groups and in patients with DM type 2 . A,C,E - baseline recording, B,D,F - during thermal stimuli.

and cardiac perfusion oscillations (region 2) (see Fig. 9A-C). To compare the diagnostic significance of the two approaches, with and without the independent filtering by the Doppler shift frequencies for each input informative parameter, we used the method of linear discriminant analysis (LDA). This method demonstrates better performance with small and limited training sets and is not susceptible to over-training. To ensure the stability of the classifier and avoid over-fitting, leave-one-out cross-validation was used. The classifiers based on the amplitudes from the selected regions demonstrated significantly better performance in comparison with those averaged over a wide frequency range. Fig. 10 shows the values of the canonical scores for the classifiers to distinguish diabetic patients from the controls, as well as delineate the two control groups, where the difference in age is apparently the most significant factor. The corresponding coefficients of the linear discriminant functions are shown in the upper part of each image. The area under the curve (AUC) of the related receiver operating characteristic was used to quantitatively compare the classifiers. The blood perfusion decomposition

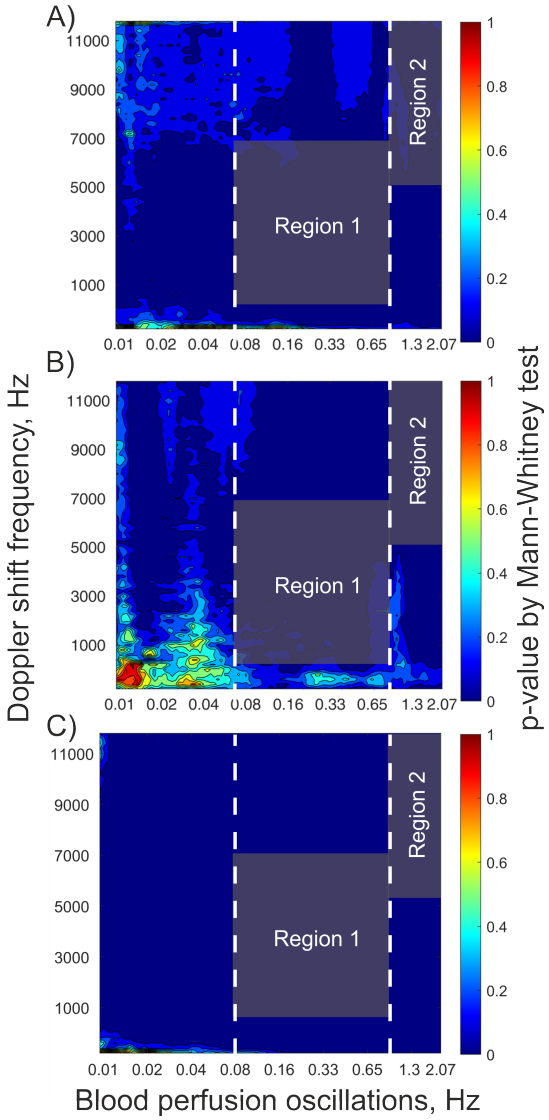

Fig. 9. The map of the p-values calculated by the Mann-Whitney U-test over all calculated amplitudes of the blood perfusion oscillations and the corresponding frequencies of the power spectra (Doppler shift frequencies) allowed us to find the regions of the amplitudes with better diagnostic values. A – Older volunteers vs Young volunteers; B – Older volunteers vs Patients; C – Young volunteers vs Patients

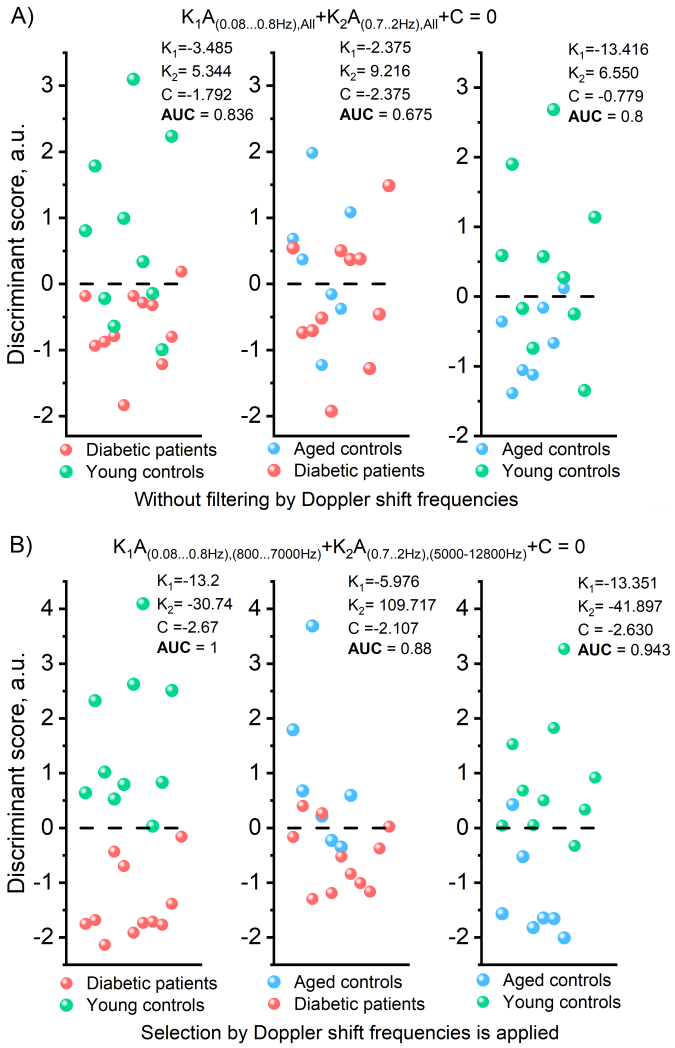

Fig. 10. Discriminant scores obtained as values of linear discriminant function. Selection by both frequencies of the blood flow oscillations and the Doppler shift frequencies allows the new signal processing technique to significantly improve the quality of the diagnostics of vascular complications in the feet of patients with DM type 2.

used, together with flexible filtering by the Doppler shift frequencies, allowed the approach of increasing the AUC for the pair of diabetic patients and young controls from 0.84 to 1, and for the pair of diabetic group and older controls from 0.68 to 0.88. The delineation of the two control groups was also improved, with a rise in AUC from 0.80 to 0.94.

Vascular changes in diabetes have been a topic of vital interest for decades. At the moment, several techniques with evaluated efficiency have been developed. Transcutaneous oximetry ($TcPO_2$) and techniques based on the use of coherent light, such as LDF and laser speckle contrast imaging (LSCI), can be accepted as the closest diagnostic technologies which can be directly compared with the presented results [59]. The application of $TcPO_2$ measurements has been demonstrated for the detection of circulatory problems leading to peripheral artery disease (PAD) and diabetic foot ulcers. Recently, it has been reported that, for the use of $TcPO_2$ for the detection of PAD, the sensitivity/specificity can reach 77.5%/75%, respectively. The reliable predictive value of diabetic foot ulcer healing by $TcPO_2$ can be estimated as 72% for sensitivity and 86% for specificity) [60]. The LSCI technique has previously been used for the detection of clinical neuropathy, with the parameters of sensitivity and specificity obtained as 75% and 85% [61], while for the prediction of healing of diabetic foot ulcers, LSCI blood perfusion measurements were suspected to be mostly inefficient [62]. For the results obtained in measurements with diabetic patients and volunteers of matched age by cross-validation (for data presented in Fig. 10B), the sensitivity and specificity of the delineation of the two groups were estimated as 70% and 78%, respectively. While the results are rather preliminary and further clinical trials are required, the estimated efficiency is at the level of the current diagnostic efficiency of similar technologies. Here, we should note that the group of diabetic volunteers did not have either

confirmed PAD or development of the diabetic foot syndrome and, rather, the presence of microvascular changes due to the course of diabetes can be supposed.

Apparently, the improvement in the quality of delineation of the groups can be explained by the more flexible selection of input parameters which are better tuned to subtle, hidden effects in the microvascular blood flow. At the anatomical level, these changes may be associated with a difference in the shape of the capillaries and the organisation of the capillary network under the factors of ageing and the development of type 2 DM. This assumption finds support in studies of capillary shapes by video capillaroscopy [63]. The article describes severe capillary shape changes in type 2 DM patients, including the giant capillaries and large inter-capillary distances. As for shape changing, twisted capillaries and coiled capillaries are reported here [64] in patients with type 2 DM as frequent complications. In the other article, it was shown that the quantity of capillaries decreases in the group of patients with type 2 DM [65]. The capillaries of diabetic patients, as a rule, have an increased diameter [66], which may also affect the shape of the resulting Doppler spectrum computed to quantify the blood flow by the LDF technique. In addition, a systematic source review of various capillary pathologic changing is shown at [67]. Nevertheless, we suppose that discovered effects in patients with type 2 DM may not only be associated with the anatomy of capillaries and the organisation of the capillary network. Functional changes in the microvessels may have as much or more to contribute to the recorded alterations in the blood perfusion parameters.

IV. Conclusions

In this paper, we introduce a new signal processing approach suitable for most modern LDF monitors. Our results suggest the achievement of greater flexibility and informativeness of the method for a range of applications in physiological studies and medical diagnostics. In a systematic way, we demonstrate how blood perfusion decomposition in narrow spectral sub-bands with subsequent flexible filtering by the Doppler shift frequencies allows information that is hidden when measured by conventional LDF monitors to be discovered and quantitatively characterised. The developed approach was validated in occlusion tests with healthy volunteers, as well as in local pressure tests rendered by a probe on the skin surface. Finally, in limited clinical trials, we demonstrate that the approach can significantly improve the diagnostic accuracy of detection of microvascular changes in the skin of the feet in patients with DM type 2, as well as age-specific changes. The obtained results show that the developed approach of LDF signal decomposition provides essential new information about blood flow and blood microcirculation and has great potential in the diagnosis of vascular complications associated with various diseases.

As a final remark, we should note that the proposed signal processing technique and the demonstrated results are of high relevance for the booming industry of wearable personalised sensors. At the moment, we observe a gradual transition of LDF measurements from table-top devices equipped with fibre-optical probes towards fibre-free, extremely compact devices with built-in, energy-efficient, single-mode VCSELs. The studied effects of the impact of low and moderate probe pressure on the recorded blood flow oscillations and their shifts in the dimension of the Doppler frequencies may improve the overall quality of the detection of vascular changes associated with ageing or type 2 DM and help in the interpretation of similar data collected from wearable devices, when the holding force will inevitably affect the results of measurements.

References

[1] D. Zhu *et al.*, "Recent progress in tissue optical clearing," *Laser Photonics Rev.*, vol. 7, no. 5, pp. 732–757, 2013.
[2] Z. Steelman *et al.*, "Light scattering methods for tissue diagnosis," *Optica*, vol. 6, no. 4, p. 479–489, 2019.
[3] R. Bonner and R. Nossal, "Model for laser Doppler measurements of blood flow in tissue," *Appl. Opt.*, vol. 20, no. 12, pp. 2097–2107, 1981.
[4] I. Fredriksson and M. Larsson, "On the equivalence and differences between laser Doppler flowmetry and laser speckle contrast analysis," *J. Biomed. Opt.*, vol. 21, no. 12, p. 126018, 2016.
[5] A. T. Forrester, "Photoelectric mixing as a spectroscopic tool," *J. Opt. Soc. Am.*, vol. 51, no. 3, pp. 253–259, 1961.
[6] Y. Yeh and H. Z. Cummins, "Localized fluid flow measurements with an He–Ne laser spectrometer," *Appl. Phys. Lett.*, vol. 4, no. 10, pp. 176–178, 1964.
[7] S. Morikawa *et al.*, "Laser Doppler measurements of localized pulsatile fluid velocity," *IEEE Trans. Biomed. Eng.*, vol. 18, no. 6, pp. 416–420, 1971.
[8] T. Tenland *et al.*, "Spatial and temporal variations in human skin blood flow," *Int. J. Microcirc. Clin. Exp.*, vol. 2, no. 2, pp. 81–90, 1983.
[9] E. G. Salerud *et al.*, "Rhythmical variations in human skin blood flow," *Int. J. Microcirc. Clin. Exp.*, vol. 2, no. 2, pp. 91–102, 1983.
[10] T. Stankovski *et al.*, "Time-frequency methods and voluntary ramped-frequency breathing: A powerful combination for exploration of human neurophysiological mechanisms," *J. Appl. Physiol.*, vol. 115, no. 12, pp. 1806–1821, 2013.
[11] A. A. Grinevich *et al.*, "Role of additive stochastic modulation of the heart activity in the formation of 0.1-hz blood flow oscillations in the human cardiovascular system," *Dokl. Biol. Sci.*, vol. 468, no. 1, pp. 106–111, 2016.
[12] M. Bračič and A. Stefanovska, "Wavelet-based analysis of human blood-flow dynamics," *Bull. Math. Biol.*, vol. 60, no. 5, pp. 919–935, 1998.
[13] A. Stefanovska *et al.*, "Wavelet analysis of oscillations in the peripheral blood circulation measured by laser Doppler technique," *IEEE Trans. Biomed. Eng.*, vol. 46, no. 10, p. 1230, 1999.
[14] T. Söderström *et al.*, "Involvement of sympathetic nerve activity in skin blood flow oscillations in humans," *Am. J. Physiol. Heart Circ. Physiol.*, vol. 284, no. 5, pp. H1638–H1646, 2003.
[15] V. V. Dremin *et al.*, "Multimodal optical measurement for study of lower limb tissue viability in patients with diabetes mellitus," *J. Biomed. Opt.*, vol. 22, no. 8, p. 085003, 2017.
[16] I. Mizeva *et al.*, "Spectral analysis of the blood flow in the foot microvascular bed during thermal testing in patients with diabetes mellitus," *Microvasc. Res.*, vol. 120, pp. 13–20, 2018.
[17] E. A. Zherebtsov *et al.*, "Combined use of laser Doppler flowmetry and skin thermometry for functional diagnostics of intradermal finger vessels," *J. Biomed. Opt.*, vol. 22, no. 4, p. 040502, 2017.
[18] A. I. Zherebtsova *et al.*, "Multimodal optical diagnostics of the micro-haemodynamics in upper and lower limbs," *Front. Physiol.*, vol. 10, p. 416, 2019.
[19] S. Komaki *et al.*, "Gingival blood flow before, during, and after clenching, measured by laser Doppler blood flowmeter: A pilot study," *Am. J. Orthod. Dentofacial Orthop.*, vol. 161, no. 1, p. 46–52, 2021.
[20] M. Miron *et al.*, "Using laser-Doppler flowmetry to evaluate the therapeutic response in dentin hypersensitivity," *Int. J. Environ. Res. Public Health*, vol. 17, no. 23, p. 8787, 2020.
[21] N. Ghouth *et al.*, "The diagnostic accuracy of laser Doppler flowmetry in assessing pulp blood flow in permanent teeth: A systematic review," *Dent. Traumatol.*, vol. 34, no. 5, pp. 311–319, 2018.
[22] E. D. Arverud *et al.*, "Microcirculation in healing and healthy achilles tendon assessed with invasive laser Doppler flowmetry," *Muscles Ligaments Tendons J.*, vol. 6, no. 1, pp. 90–96, 2016.

[23] T. Mücke *et al.*, "Identification of perioperative risk factor by laser-Doppler spectroscopy after free flap perfusion in the head and neck: A prospective clinical study," *Microsurgery*, vol. 34, no. 5, pp. 345–351, 2014.

[24] K. Merz *et al.*, "Cutaneous microcirculatory assessment of the burn wound is associated with depth of injury and predicts healing time," *Burns*, vol. 36, no. 4, pp. 477–482, 2010.

[25] W. Iwasaki *et al.*, "Detection of site-specific blood flow variation in humans during running by a wearable laser Doppler flowmeter," *Sensors (Basel)*, vol. 15, no. 10, p. 25507–25519, 2015.

[26] A. Ishimaru, *Wave propagation and scattering in random media: Multiple scattering, turbulence, rough surfaces, and remote sensing*. San Diego, CA: Academic Press, 1978, vol. 2.

[27] S. Wojtkiewicz *et al.*, "Estimation of scattering phase function utilizing laser Doppler power density spectra," *Phys. Med. Biol.*, vol. 58, no. 4, pp. 937–955, 2013.

[28] S. Wojtkiewicz et al, "Evaluation of algorithms for microperfusion assessment by fast simulations of laser Doppler power spectral density," *Phys. Med. Biol.*, vol. 56, no. 24, p. 7709–7723, 2011.

[29] A. Liebert *et al.*, "Decomposition of a laser-Doppler spectrum for estimation of speed distribution of particles moving in an optically turbid medium: Monte Carlo validation study," *Phys. Med. Biol.*, vol. 51, no. 22, p. 5737–5751, 2006.

[30] A. N. Obeid, "*In vitro* comparison of different signal processing algorithms used in laser Doppler flowmetry," *Med. Biol. Eng. Comput.*, vol. 31, no. 1, pp. 43–52, 1993.

[31] X. Qu *et al.*, "Improvement of the detection of human pulpal blood flow using a laser Doppler flowmeter modified for low flow velocity," *Arch. Oral Biol.*, vol. 59, no. 2, pp. 199–206, 2014.

[32] T. Odor *et al.*, "Effect of wavelength and bandwidth on the clinical reliability of laser Doppler recordings," *Dent. Traumatol.*, vol. 12, no. 1, pp. 9–15, 1996.

[33] Y. Y. Chen *et al.*, "Adaptive processing bandwidth adjustment for laser Doppler flowmetry," *Med. Biol. Eng. Comput.*, vol. 42, no. 3, pp. 277–281, 2004.

[34] A. Humeau-Heurtier *et al.*, "Multiscale compression entropy of microvascular blood flow signals: Comparison of results from laser speckle contrast and laser Doppler flowmetry data in healthy subjects," *Entropy*, vol. 16, pp. 5777–5795, 2014.

[35] M. Meinke *et al.*, "Frequency weighted laser Doppler perfusion measurements in skin," *Laser Phys. Lett.*, vol. 4, no. 1, pp. 66–71, 2007.

[36] I. Fredriksson *et al.*, "Model-based quantitative laser Doppler flowmetry in skin," *J. Biomed. Opt.*, vol. 15, no. 5, p. 057002, 2010.

[37] S. Wojtkiewicz *et al.*, "Assessment of speed distribution of red blood cells in the microvascular network in healthy volunteers and type 1 diabetes using laser Doppler spectra decomposition," *Physiol. Meas.*, vol. 35, no. 2, p. 283, 2014.

[38] G. Wang *et al.*, "Exploring the relationship between the speed-resolved perfusion of blood flux and hrv following different thermal stimulations using MSE and MFE analyses," *PLOS ONE*, vol. 14, no. 6, p. e0217973, 2019.

[39] H. Jonasson *et al.*, "Validation of speed-resolved laser Doppler perfusion in a multimodal optical system using a blood-flow phantom," *J. Biomed. Opt.*, vol. 24, no. 9, p. 095002, 2019.

[40] M. J. Leahy *et al.*, "Principles and practice of the laser-doppler perfusion technique," *J. Health Care Technol.*, vol. 7, no. 2-3, pp. 143–162, 1999.

[41] A. P. Shepherd, *Laser-Doppler blood flowmetry*. Boston, MA: Springer US, 1990.

[42] J. H. Klaessens *et al.*, "Monitoring cerebral perfusion using near-infrared spectroscopy and laser Doppler flowmetry," *Physiol. Meas.*, vol. 24, no. 4, p. N35–N40, 2003.

[43] P. Goupillaud *et al.*, "Cycle-octave and related transforms in seismic signal analysis," *Geoexploration*, vol. 23, no. 1, pp. 85–102, 1984.

[44] B. D. Tran *et al.*, "Exercise and repeated testing improves accuracy of laser Doppler assessment of microvascular function following shortened (1-minute) blood flow occlusion," *Microcirculation*, vol. 23, no. 4, pp. 293–300, 2016.

[45] G. E. Nilsson *et al.*, "Evaluation of a laser Doppler flowmeter for measurement of tissue blood flow," *IEEE Trans. Biomed. Eng.*, vol. 27, no. 10, pp. 597–604, 1980.

[46] A. N. Obeid *et al.*, "A critical review of laser Doppler flowmetry," *J. Med. Eng. Technol.*, vol. 14, no. 5, pp. 178–181, 1990.

[47] Y. Ti and W.-C. Lin, "Effect of probe contact pressure on *in vivo* optical spectroscopy," *Opt. Express*, vol. 16, no. 6, pp. 4250–4262, 2008.

[48] A. Popov *et al.*, "Influence of probe pressure on diffuse reflectance spectra of human skin measured *in vivo*," *J. Biomed. Opt.*, vol. 22, no. 11, p. 110504, 2017.

[49] I. Mizeva *et al.*, "Optical probe pressure effects on cutaneous blood flow," *Clin. Hemorheol. Microcirc.*, vol. 72, no. 3, pp. 259–267, 2019.

[50] J.-L. Cracowski and M. Roustit, "Current methods to assess human cutaneous blood flow: An updated focus on laser-based-techniques," *Microcirculation*, vol. 23, no. 5, pp. 337–344, 2016.

[51] Y.-K. Jan *et al.*, "Skin blood flow response to locally applied mechanical and thermal stresses in the diabetic foot," *Microvasc. Res.*, vol. 89, pp. 40–46, 2013.

[52] S. Bergstrand *et al.*, "Blood flow measurements at different depths using photoplethysmography and laser Doppler techniques," *Skin Res. Technol.*, vol. 15, no. 2, pp. 139–147, 2009.

[53] V. Kalchenko *et al.*, "Visualization of blood and lymphatic vessels with increasing exposure time of the detector," *Quantum Electron.*, vol. 43, no. 7, pp. 679–682, 2013.

[54] D. Kerjaschki, "The lymphatic vasculature revisited," *J. Clin. Invest.*, vol. 124, no. 3, pp. 874–877, 2014.

[55] V. Kalchenko *et al.*, "Label free *in vivo* laser speckle imaging of blood and lymph vessels," *J. Biomed. Opt.*, vol. 17, no. 5, p. 050502, 2012.

[56] I. Meglinski *et al.*, "Towards the nature of biological zero in the dynamic light scattering diagnostic techniques," *Dokl. Phys.*, vol. 58, no. 8, pp. 323–326, 2013.

[57] H. N. Mayrovitz and J. A. Leedham, "Laser-Doppler imaging of forearm skin: Perfusion features and dependence of the biological zero on heat-induced hyperemia," *Microvasc. Res.*, vol. 62, no. 1, pp. 74–78, 2001.

[58] V. Dremin *et al.*, "Influence of blood pulsation on diagnostic volume in pulse oximetry and photoplethysmography measurements," *Appl. Opt.*, vol. 58, no. 34, pp. 9398–9405, 2019.

[59] V. Fejfarová *et al.*, "Stimulation TcPO2 testing improves diagnosis of peripheral arterial disease in patients with diabetic foot," *Front. Endocrinol.*, vol. 12, p. 1637, 2021.

[60] Z. Wang *et al.*, "A systematic review and meta-analysis of tests to predict wound healing in diabetic foot," *J. Vasc. Surg.*, vol. 63, no. 2, pp. 37S–45S, 2016.

[61] P. R. Vas and G. Rayman, "The rate of decline in small fibre function assessed using axon reflex-mediated neurogenic vasodilatation and the importance of age related centile values to improve the detection of clinical neuropathy," *PLOS ONE*, vol. 8, no. 7, p. e69920, 2013.

[62] O. A. Mennes *et al.*, "The association between foot and ulcer microcirculation measured with laser speckle contrast imaging and healing of diabetic foot ulcers," *J. Clin. Med.*, vol. 10, no. 17, p. 3844, 2021.

[63] G. Maldonado *et al.*, "Nailfold capillaroscopy in diabetes mellitus," *Microvasc. Res.*, vol. 112, p. 41–46, 2017.

[64] A. Rajaei *et al.*, "Nailfold capillaroscopy findings in diabetic patients (a pilot cross-sectional study)," *Open J. Pathol.*, vol. 5, no. 2, pp. 65–72, 2015.

[65] C. H. Chang *et al.*, "Use of dynamic capillaroscopy for studying cutaneous microcirculation in patients with diabetes mellitus," *Microvasc. Res.*, vol. 53, no. 2, p. 121–127, 1997.

[66] I. Fredriksson and M. Larsson, "Vessel packaging effect in laser speckle contrast imaging and laser Doppler imaging," *J. Biomed. Opt.*, vol. 22, no. 10, p. 106005, 2017.

[67] J. Ciaffi *et al.*, "Nailfold capillaroscopy in common non-rheumatic conditions: A systematic review and applications for clinical practice," *Microvasc. Res.*, vol. 131, p. 104036, 2020.